JREE: Vol. 9, No. 1, (Winter 2022) 23-36

Journal of Renewable Energy and Environment

Journal Homepage: www.jree.ir

Materials and Energy Research Center

MERC

Research Article

Assessment of Effect of Different Parameters on Temperature Distribution in Chemical Looping Combustor: Experimental and Numerical Approaches

Mohamed A. Barakat, Tamer Mohamed Ismail, Sayed Ibrahim Abdel-Mageed, Khaled Ramzy *

Department of Mechanical Engineering, Faculty of Engineering, Suez Canal University, Ismailia, Egypt.

PAPER INFO

Paper history:
Received: 26 January 2021
Revised in revised form: 15 March 2021
Scientific Accepted: 12 April 2021
Published: 07 November 2021

Keywords:
CO_2 Capture,
Chemical Looping Combustion,
Solid Fuel,
Gaseous Fuel,
Nickel Powder,
Modelling

ABSTRACT

The greenhouse problem has a significant effect on our communities, health, and climate. So, the capturing techniques for CO_2 remain the focus of attention these days. In this work, a Chemical Looping Combustor (CLC) was designed and fabricated with the major geometric sizes at the Faculty of Engineering, Suez Canal University. The system involves two interconnected fluidized beds. Nickel powder with 150 µm diameter as well as brown coal and liquefied petroleum gas were used as oxygen carrier, solid fuel, and gaseous fuel, respectively. The temperature distributions along the fuel reactor for LPG flow rates of 11 and 18 LPM with and without using nickel powder as well as using preheated reactor were discussed and evaluated. The effects of brown coal diameter change with and without using nickel powder were studied. The CO and CO_2 concentrations at combustion gases with and without using nickel powder were conducted for LPG and brown coal fuels. A mathematical model was used to simulate the combustion in CLC using combustion and energy code. The obtained results showed that using nickel powder improved the combustion process and in case of using LPG, the flame color changed to blue which is the color of the complete combustion flame. The CO was reduced by 48.4 % and CO_2 was augmented by 66.5 %. In case of using brown coal as solid fuel, CO was reduced by 53.7 % and CO_2 was increased by 71.9 %. Finally, there is good agreement between the experimental and numerical results based on the determination coefficient.

https://doi.org/10.30501/jree.2021.269946.1182

1. INTRODUCTION

Recently, the greenhouse effect has been the focus of attention of many scientists. Close to the years 1910-1940 and from 1970 to 2000, the earth's surface temperature increased by 0.35 °C and 0.55 °C, respectively. Based on the data recorded by global climate change organizations, the last decade has been the warmest [1]. The effect of the global warming problem is not limited to increasing the earth's surface temperature; however, as a result of this problem, scientists expect a steady increase in ice melting and increase in sea level above the normal. Many scientists today agree that an industrial greenhouse effect is the main cause of global warming such as combustion of fossil fuels and emissions of CO_2 [2]. Consequently, it is necessary to separate and store the CO_2 produced from combustion processes. A possible solution is to produce a pure stream of CO_2 from fossil fuels combustion and store it. This concept can be used as a long-term interim solution until the renewable energy sources can replace the traditional combustion systems. One of the newest technologies in this respect is called chemical looping combustion. It is a novel combustion process for gaseous or solid fuels, producing a pure stream of CO_2 [3].

Carbon capture and storage technology can be used to reduce the emitted carbon dioxide into the atmosphere in many fields of industry and power generation. If this technology is successfully used in different industrial areas and power plants, 57 % of CO_2 emissions can be reduced [4]. Driven by the global trend to reduce carbon dioxide in industrial emissions, many scientists investigated different methods of carbon dioxide capture in industrial application. However, the main problem is that carbon dioxide capture is very expensive and exceeds the cost of capturing one ton of carbon dioxide at 12 dollars. Carbon dioxide capturing at power plants reduces their efficiency by 10 ± 2 % [5].

Chemical looping combustion is the unmixed combustion technique because the fuel and the air do not have a direct reaction. Combustion occurs without air contact with fuel, where oxygen is separated from the air by a metal powder, called oxygen-carriers; therefore, the process of combustion is carried out by oxygen only and carbon dioxide can be captured with high efficiency. In chemical looping combustion, oxygen-carrier particles are run between two reactors, as shown in Figure 1.

In the first reactor, air flows from the bottom where the oxidation of particles occurs. This reactor is usually called an

*Corresponding Author's Email: kh.ramzy2005@eng.suez.edu.eg (Kh. Ramzy)
URL: https://www.jree.ir/article_139804.html

Please cite this article as: Barakat, M.A., Ismail, T.M., Abdel-Mageed, S.I. and Ramzy, Kh., "Assessment of effect of different parameters on temperature distribution in chemical looping combustor: Experimental and numerical approaches", ***Journal of Renewable Energy and Environment (JREE)***, Vol. 9, No. 1, (2022), 23-36. (https://doi.org/10.30501/jree.2021.269946.1182).

air-reactor. Then, the metal powder is transported through a ring seal to the second reactor where the fuel is inserted and this reactor is called the fuel-reactor [6-7]. The fuel and the available oxygen in the oxygen-carrier particles react according to Equation 1.

$$(2n + m)Me_xO_{y+1} + C_nH_{2m} \rightarrow (2n + m)Me_xO_y` + nCO_2 + mH_2O \quad (1)$$

Oxygen-carrier is reduced in fuel reactor and the metal powder is transferred to the air reactor to be oxidized, as shown in Equation 2.

$$2Me_xO_y + O_2 \rightarrow 2Me_xO_{y+1} \quad (2)$$

where Me_xO_{y+1} is the oxidized metal-powder and Me_xO_y is the reduced metal powder. Therefore, the objective of this process is to transport oxygen to the fuel reactor without any direct loss of efficiency and without nitrogen-dilute gas in the reaction results. Following the condensation of water and cleaning of the exhaust from impurities such as So_x, a pure stream of CO_2 is ready to be transported to a suitable location for storage [8-9]. Lewis and Gilliland put forward the principle of chemical looping combustion first [10-11].

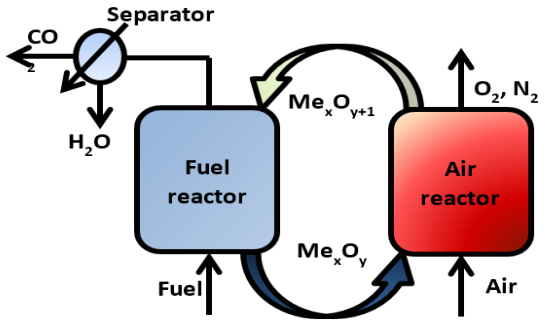

Figure 1. Schematic diagram of the chemical looping combustion process

Chemical looping combustion was first coined by Ishida et al. [11] and they recognized the concept of CLC system to capture CO_2 from fossil fuels. Lyngfelt et al. presented the first chemical looping combustion design based on the circulating fluidized bed principle [6]. More different materials have been investigated as oxygen carrier materials for use in CLC technology, especially the active oxides of iron, nickel, copper, and manganese [12]. In the beginning of the year 2011, it was reported that operation for more than 4000 h was completed in 12 different units [13] using gaseous fuels. Through the last few years, solid fuel has received a greater focus than liquid fuels, but the latter have been tested in relatively small lab units [14]. Until the year 2012, reports on nearly 120 hours of operation with three different oxygen carriers have been submitted [15] and more studies have been performed on solid fuel [16]. Due to the chemical looping combustion importance, it is important to make a comparison between different types of fuel.

Therefore, the main objectives of the present study are to design and fabricate a chemical looping combustor; to compare the combustion of gaseous and solid fuels in the chemical looping combustor' to investigate the temperature distribution along the fuel reactor using gaseous and solid fuels before and after applying CLC technology. The CO and CO_2 concentrations in combustion gases with and without using nickel powder were given for LPG and brown coal fuels. The temperature distribution along the fuel reactor for LPG flow rates of 11 and 18 LPM with and without using nickel powder as well as using preheated reactor will be discussed and evaluated.

Also, this study presents the experimental results of temperature distribution along the fuel reactor for brown coal of different diameters with and without using nickel powder. In addition, a mathematical model was developed to simulate the combustion in CLC using combustion and energy code. This code investigates the concentration of gases in emissions and temperature distribution in both gas and solid phases. The experimental and simulated results were validated according to the statistical methods such as the coefficient of determination R^2 as follows.

2. EXPERIMENTAL SETUP

2.1. Design of CLC reactor

This section presents the design of the CLC combustor with its main parts and dimensions. The chemical looping combustor was designed and fabricated at the combustion lab, Faculty of Engineering, Suez Canal University. The CLC system consists of the air reactor with a height of 2.67 m and an internal diameter of 0.09 m. The air reactor is connected to the fuel reactor with a height of 1.25 m and an internal diameter of 0.2 m. The particles flow upward in the air reactor with the inlet air and can be collected by the cyclone at the top of the CLC system. Two butterfly valves are used for measuring solid circulation flux. A photograph and a schematic diagram of the chemical looping combustor system with its main geometric sizes are shown in Figure 2.

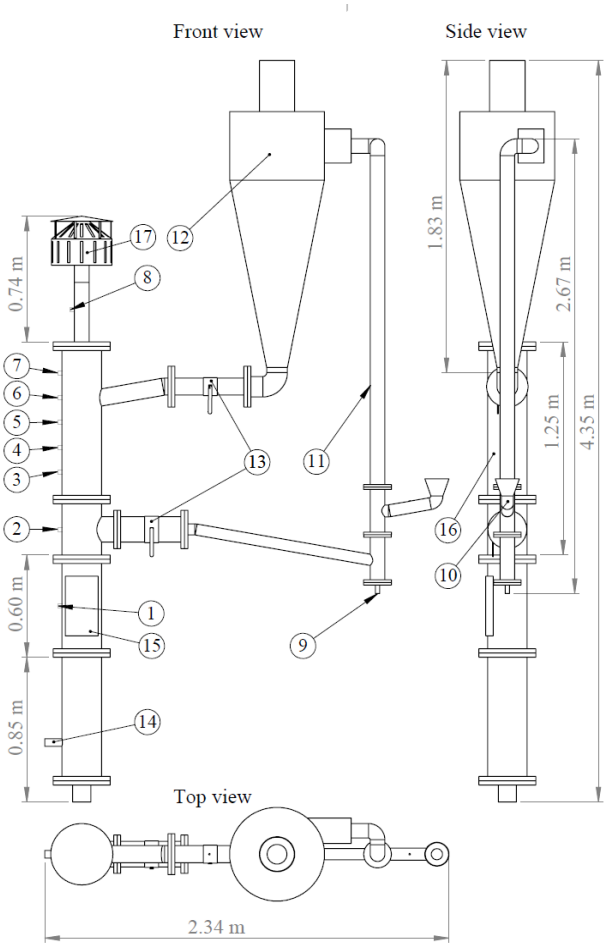

(a)

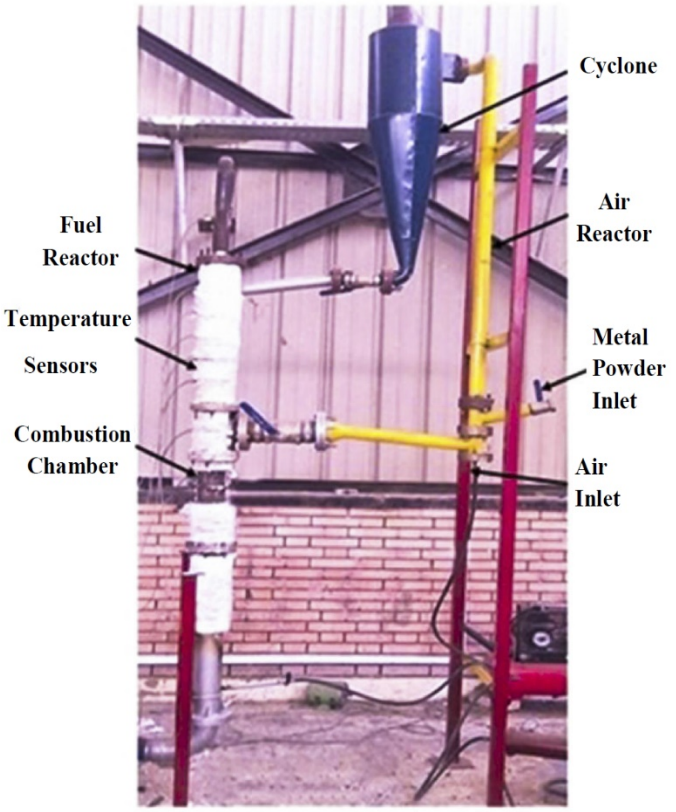

(b)

Figure 2. (a) Schematic diagram and (b) photograph of chemical looping combustion (CLC) system, where T is thermocouple sensors, 1- air inlet, 2- metal powder inlet, 3- air reactor, 4- cyclone, 5- butterfly valves, 6- burner, 7- combustion chamber, 8- fuel reactor and 9- chimney

2.2. Oxygen carrier selection

The selection of oxygen carrier is one of the most important aspects for designing the CLC system. There are many important factors to be considered when choosing an oxygen carrier. These factors include high reactivity in both cases of reduction by fuel gas and oxidation by oxygen in the air, oxygen transfer capacity, cost, environmental impacts, thermodynamic properties, and melting point. Researchers found that some oxide systems of the transition metals, Fe, Cu, Co, Mn, and Ni could be used as oxygen carriers [17, 18]. There are many experimental investigations of different oxygen carriers.

Nakano et al. [19] performed an experimental work using Fe_2O_3 with Al_2O_3 and Fe_2O_3 with Ni as support using a thermogravimetric analyzer. In addition, they presented a CLC reactor and a fixed bed reactor with gas chromatography [20]. Mattisson and Lyngfelt investigated iron ore, Fe_2O_3/Al_2O_3, and Fe_2O_3/MgO in fixed bed [21].

Also, different oxides of nickel, copper, cobalt, and manganese supported by aluminum oxide were studied by Mattisson et al. [22] for methane. From the previous studies, it can be noticed that the reaction rates during oxidation and reduction varied in a wide range depending upon the metal oxide used as well as reaction parameters. In general, nickel-based carriers appear to have the highest reduction reactivity compared to iron; manganese and copper based carriers have not been studied to the same extent. Therefore, nickel was used as metal powder in the CLC system under investigation.

2.3. Uncertainty analysis

Uncertainty in measurement is the doubt regarding the result of any measurement [23]. The analysis of experimental uncertainty was done and evaluated according to Holman [24] and Ismail et al. [25]. The minimum experimental error was equal to the ratio between its least count and the minimum recorded value of the measured output. All values were smaller than the obtained data and found to be within the allowable range of the measurements. Table 1 shows the uncertainty analysis for the measured parameters during experiments.

Table 1. Uncertainty analysis of the measured parameters

Parameter	Range	Accuracy	Uncertainty
Thermocouple K-type			
Temperature	0 °C to 1300 °C	± 2.2 °C or ± 0.25 %	± 0.043 %
Compact combustion analyzer			
Carbon dioxide	0-60 %	± 0.3	± 0.013 %
Carbon monoxide	0-2000 ppm And 4000 ppm max for 15 min	± 10 ppm ± 5 %	± 0.09 %
Rotameter			
Volume flow rate	1.2-18 LPM	-	± 2.7 %

2.4. Experimental setup for using gaseous fuel

In order to determine the effect of using CLC technology, the fuel should be combusted traditionally and the results before and after applying CLC technology need to be compared. The lower and upper explosive limits for gaseous fuel should be measured based on the system conditions. The minimum concentration of a particular combustible gas or vapor necessary to support its combustion in air is defined as the Lower Explosive Limit (LEL) for that gas. Below this level, the mixture is too "lean" to burn. The maximum concentration of a gas or vapor that burns in the air is defined as the Upper Explosive Limit (UEL). Above this level, the mixture is too "rich" to burn. In this study, Liquid Petroleum Gas (LPG) was used as gaseous fuel consisting of 60 % Propane (C_3H_8) and 40 % butane (C_4H_{10}), with a heating value equal to 46.1 MJ/kg [26]. The lower and upper explosive limits and stoichiometry percentage of Propane and Butane are shown in Table 2.

Table 2. Lower and upper explosive limits and stoichiometry percentage

Gas	LEL	UEL	Stoichiometry
Propane	2.1 %	9.5 %	4.016 %
Butane	1.8 %	8.4 %	3.135 %
All concentrations in percentage by volume			

A half HP blower with an airflow rate of 480 LPM was used as an air source for traditional combustion. Flammability limits of mixtures of several combustible gases can be measured using Le Chatelier's mixing rule for combustible volume fractions Xi using the following Equations [27].

$$LEL_{mix} = \frac{1}{\Sigma \frac{Xi}{LEL\,i}} \quad (3)$$

$$UEL_{mix} = \frac{1}{\Sigma \frac{X_i}{UEL_i}} \quad (4)$$

$$Stoichiometry_{mix} = \frac{1}{\Sigma \frac{X_i}{stoich_i}} \quad (5)$$

From the calculation above and at the air flow rate of 480 LPM, the minimum amount of fuel (Q_{min}), the maximum amount of fuel (Q_{max}), and the best ratio between the air and fuel used (Q_{stoich}) are shown in Table 3.

Table 3. Lower and upper explosive limits and stoichiometry percentage for LPG at the air flow rate of 480 LPM

Gas	Q_{min} (LPM)	Q_{max} (LPM)	Q_{stoich} (LPM)
LPG	9.64	47.629	17.98

The Q_{stoich} fuel ratio was used in experiments because due to its higher temperature than Q_{min} and lower toxic exhaust than Q_{max}. For stoichiometric combustion, Q_{fuel} =18 LPM and this flow rate consists of 40 % Butane and 60 % Propane.

$$C_3H_8 + 5\ O_2 \rightarrow 3\ CO_2 + 4\ H_2O \quad (6)$$

$$C_4H_{10} + 6.5\ O_2 \rightarrow 4\ CO_2 + 5\ H_2O \quad (7)$$

According to Equations (6) and (7), it can be noticed that 38.822×10^{-3} and 34.207×10^{-3} mole O_2 / sec are required for Propane and Butane, respectively. In order to calculate the required amount of nickel powder flow rate, the amount of needed oxygen to burn LPG components should be 73.029×10^{-3} mole/sec to burn the LPG flow rate of 18 LPM.

2.5. Experimental setup for use in solid fuel

A batch system was used by burning 300 g of brown coal with proximate analysis, as shown in Table 4. In order to calculate the required amount of nickel powder flow rate, the amount of needed oxygen to burn 300 g of brown coal experiments should be calculated. The proximate analysis for 300 g of brown coal used in experiments is shown in Table 5. From the mass percentage of the volatile matter components shown in Table 6, the required oxygen for burning combustible volatile matter can be calculated.

Table 4. Proximate analysis for brown coal

Element	Mass percent (%)
Fixed carbon (C)	39
Moisture (H_2O)	15
Volatile matter	29
Ash	17

Table 5. Proximate analysis for 300 g of brown coal

Element	Mass percent (%)	Mass for 300 g (g)	g/mole	Number of moles
Fixed carbon (C)	39	117	12	9.75
Moisture (H_2O)	15	45	18	2.5
Volatile matter	29	87	-	-
Ash	17	51	-	-

Table 6. Mass percentage for 87 g of volatile matter components

Element	Mass percent (%)	g	g/mole	Number of moles
H_2	20	17.4	2	8.7
CO	14	12.18	28	0.435
CH_4	15	13.05	16	0.82
S	1	0.87	32	0.027
N_2	5	4.35	28	0.16
O_2	24	20.88	32	0.65
CO_2	9	7.83	44	0.18
H_2O	12	10.44	18	0.58

The combustion equations of volatile matter elements are as follows:

$$8.7\ H_2 + 4.35\ O_2 \rightarrow 8.7\ H_2O \quad (8)$$

$$0.435\ CO + 0.2175\ O_2 \rightarrow 0.435\ CO_2 \quad (9)$$

$$0.82\ CH_4 + 1.64\ O_2 \rightarrow 0.82\ CO_2 + 1.64\ H_2O \quad (10)$$

$$0.027\ S + 0.027\ O_2 \rightarrow 0.027\ SO_2 \quad (11)$$

$$0.16\ N_2 + 0.32\ O_2 \rightarrow 0.32\ NO_2 \quad (12)$$

$$9.75\ C + 9.75\ O_2 \rightarrow 9.75\ CO_2 \quad (13)$$

$$32.609\ Ni + 16.3045\ O_2 \rightarrow 32.609\ NiO \quad (14)$$

According to Equations (9-13), the required oxygen for burning combustible volatile matter is equal to 6.5545 mole of O_2 and 9.75 moles of oxygen required for burning 117 g of fixed carbon. From this calculation, all the required moles of O_2 are equal to 16.3045 moles to burn 300 g of brown coal. From Equation (14), it can be noticed that 1913.82 g nickel is needed for burning 300 g of coal. From experiments, it can be noted that complete combustion with 300 g of coal takes 10 to 12 minutes. Assuming that combustion rate is constant, 2.66 to 3.2 g of nickel per the second path are required through the combustion chamber.

3. MATHEMATICAL MODELLING OF THE FUEL REACTOR

The mathematical model gives a simulation of combustion in CLC using combustion and energy code. CFD techniques offer the capacity of studying a system under conditions over its limits. In the combustion process, the simulation uses less advanced technology to study the solid, gas phase and temperature distribution of matter, thus greatly saving the calculation requirements. The mathematical model is built based on the conservation of a coupled transport equation and the equation of state of the fluid system. For obtaining a time- and grid-independent solution, the presented simulations were performed with a time step of 2×10^{-3} s and a space step of 0.1 mm. The combustion process was launched by the gas burner. More details of the current model can be found in the supplementary materials. The previously described mathematical model was evaluated based on the coefficient of determination, R^2. This statistical value can be used to test the linear relationship between the calculated and measured values; its value should be as close to unity as possible and is given by the following equation [28]:

$$R^2 = 1 - \frac{\text{Error between experimentaland predicted results}}{\text{Experimental result deviation}} \quad (15)$$

$$R^2 = 1 - \frac{\sum(E_m - E_c)^2}{\sum(E_m - \overline{E}_m)} \quad (16)$$

where E_m and E_c are the measured and calculated values, respectively. The term $\overline{E}_m$ in Equation (16) is the average measured value which can be defined as follows [28]:

$$\overline{E}_m = \frac{\sum_{i=1}^{n_p} E_m}{n_p} \quad (17)$$

where n_p is the number of experimental points.

4. RESULTS AND DISCUSSION

4.1. Gaseous fuel (LPG)

This section provides the results of temperature distribution along the fuel reactor of LPG as a gaseous fuel. The temperature was measured using K-type thermocouple with a data acquisition system. Also, this section gives the concentration measurements of CO and CO_2 in combustion exhaust in three different cases.

4.1.1. Experimental and simulated results for LPG without nickel powder

After preparing CLC reactor along the fuel reactor, a volume flow rate less than the stoichiometric was measured and recorded, as shown in Figure 3. This figure shows that the maximum recorded temperature was 576 ºC at T_1 and the temperature gradually decreased to 288 ºC at T_8. The simulated results of temperature distribution are shown in Figure 4. After preparing the CLC reactor and adjusting the volume flow rate to 18 LPM, the temperature distribution along the fuel reactor was measured and plotted, as shown in Figure 5. From the figure evaluation, it can be noticed that the maximum-recorded temperature was 824 ºC and recorded by T_1. The temperature distribution starts decreasing gradually along the fuel reactor to reach 417 ºC at T_8. The simulated results of temperature distribution along the fuel reactor for the LPG volume flow rate of 18 LPM are shown in Figure 6. The red region in the simulated results represents the highest temperature and blue region represents the lowest temperature in the domain. It is clearly seen in these figures that the high-temperature region occurs in the bottom of the reactor and decreases gradually along the reactor length.

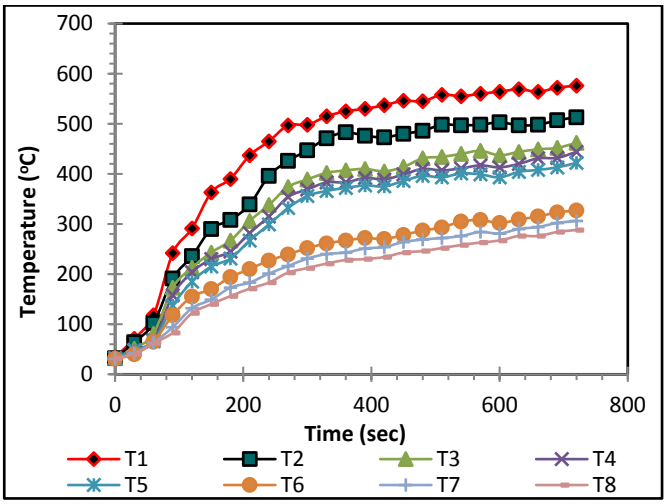

Figure 3. Experimental results of temperature distribution along the fuel reactor for LPG (Q = 11 LPM), without using nickel powder

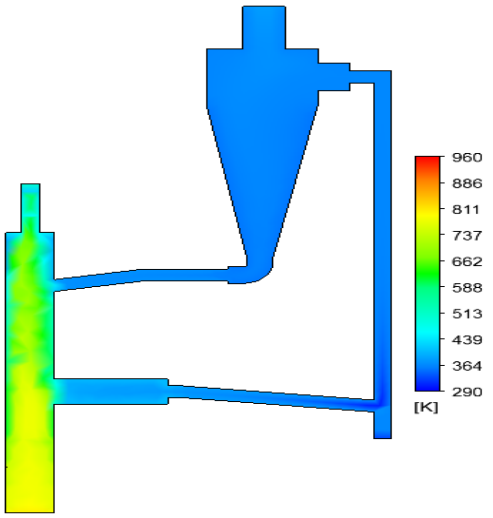

Figure 4. Simulated results of temperature distribution for LPG (Q = 11 LPM) without using nickel powder

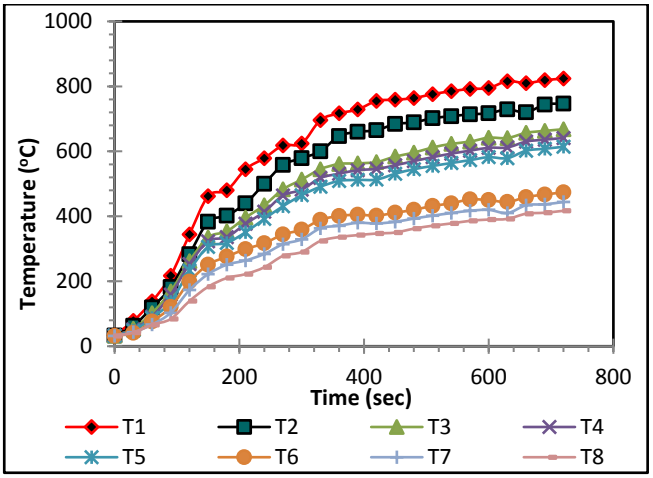

Figure 5. Experimental temperature distribution along the fuel reactor for LPG without using nickel powder

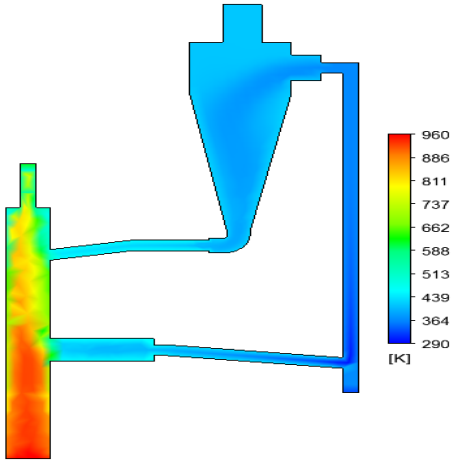

Figure 6. Simulated results of temperature distribution for LPG without using nickel powder

4.1.2. Comparison between experimental and simulated results for different flow rates of LPG

The comparison between the temperature distribution in the combustion chamber (T_1) for LPG flow rates of 11 and 18 LPM is shown in Figure 7. In the experiments, the proportion of gases emitted before and after the use of nickel powder is compared; therefore, the perfect LPG volume flow rate should be chosen to be used in all subsequent experiments. The simulated results of temperature distribution and different values of flow rates for LPG are shown in Figure 8. It was observed that the flow rate of 18 LPM was perfect and the temperature at the beginning of the experiments was less than the requirement of the reduction process of nickel powder. Therefore, it is necessary to preheat the reactor before starting the combustion process for obtaining high temperature. The experimental results of temperature distribution along the preheated fuel reactor for 18 LPM of LPG are shown in Figure 9. From this figure, it is clear that there is a high-temperature distribution along the fuel reactor at the beginning of the experiment and this is sufficient for nickel reduction, and the maximum recorded temperature was 1079 °C. For this reason, all the following experiments for gaseous fuel were carried out with 18 LPM after preheating the reactor. Also, the simulated results of the LPG volume flow rate of 18 LPM with preheated reactor are shown in Figure 10. From the analysis of these figures, it can be concluded that the temperature distribution is very crucial which occurs by different colors in the model domain.

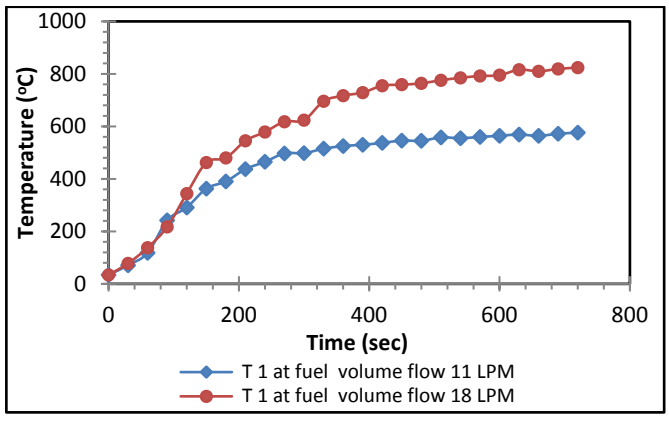

Figure 7. Comparison between the temperature distribution in the combustion chamber (T_1) at different LPG volume flow rates (Q = 11 and 18 LPM)

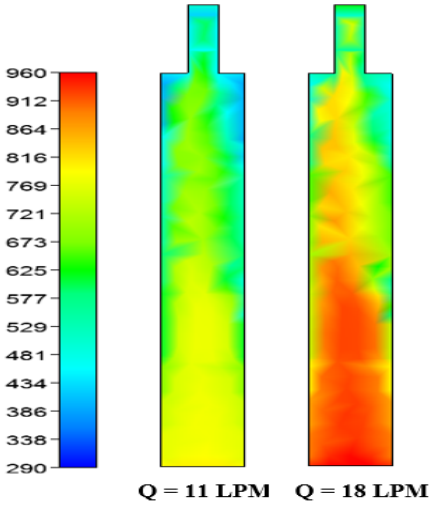

Figure 8. Simulated results of temperatures along the fuel reactor for different LPG volume flow rates (Q = 11 and 18 LPM)

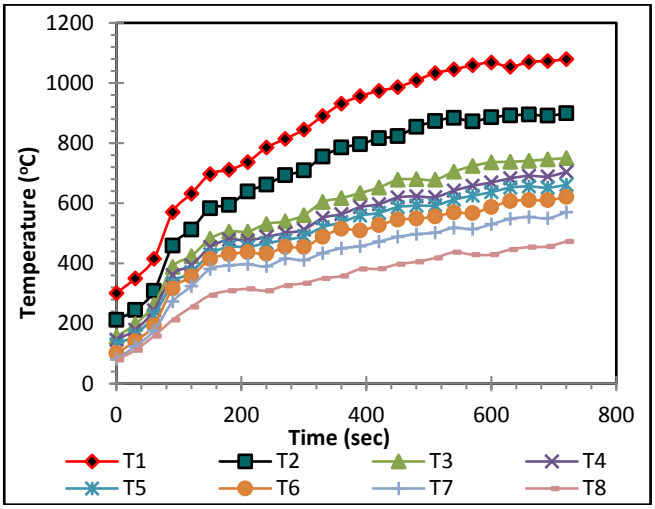

Figure 9. Experimental temperature distribution along the fuel reactor for LPG, preheated reactor without using nickel powder

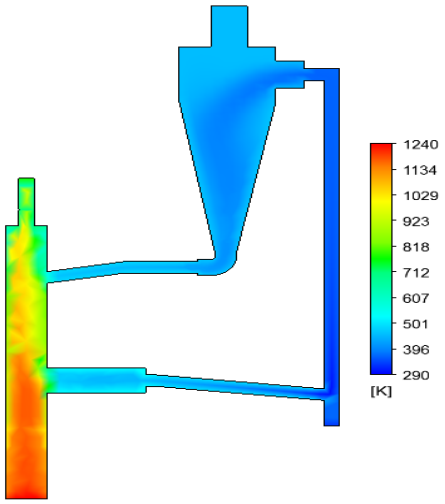

Figure 10. Simulated results of temperature distribution with LPG and preheated reactor without using nickel powder

4.1.3. Validation for using LPG without nickel powder

Figure 11 shows a comparison between experimental and simulated results of temperature distribution for preheated fuel

reactor using LPG with a flow rate of 18 LPM without using nickel powder. Based on the analysis of this figure, it is clear that the values for experimental results and simulated results are different. This is due to the adiabatic system and the laminar flow. Therefore, there is no leakage of heat in the numerical system; in contrast, there is a leakage in the heat in the practical experiments. Moreover, the accuracy in measuring instruments is not ideal. The coefficient of determination (R^2) for the experimental and simulated results values of the LPG equals 80.83 %.

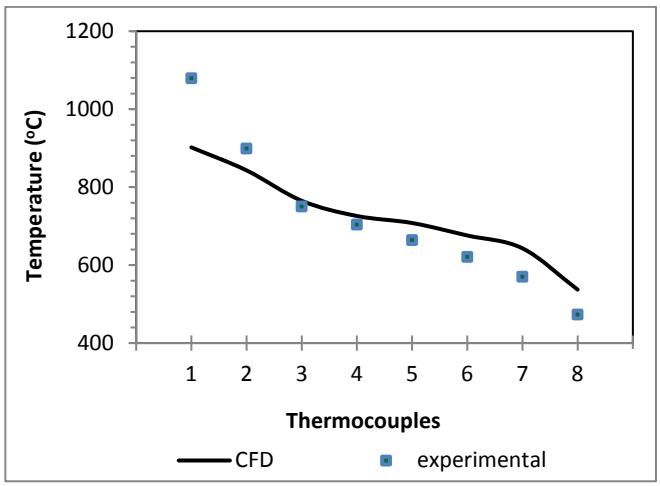

Figure 11. Experimental and simulated results of temperature distribution for LPG and preheated reactor without using nickel powder

4.1.4. Experimental concentrations of CO and CO_2 for gaseous fuel

Table 7 shows the operating conditions of carbon monoxide and carbon dioxide concentrations measurement for different cases with using gaseous fuel (LPG).

Table 7. Operating conditions of CO and CO_2 concentrations of measurement experiments using LPG

Case	Combustion method	The reactor used in combustion	The used amount of nickel
Gaseous fuel (18 LPM of LPG)			
Case # 1	Conventional combustion	The fuel reactor after separating it from the air reactor	without using nickel powder
Case # 2	CLC combustion technology	CLC system (fuel reactor and air reactor)	90 g
Case # 3			135 g and 45 g supplementation

Case # 1: Gaseous fuel, without nickel powder

In the experimental work, the concentration of carbon monoxide and carbon dioxide in the combustion exhaust emissions was measured using the gas analyzer. Figure 12 shows the concentrations of CO and CO_2 emissions for gaseous fuel without using metal powder. From the analysis of this figure, it is clear that the concentration of carbon monoxide increased continuously until the end of the experiment. In contrast, the concentration of carbon dioxide was reduced significantly throughout the experiment. The average values of the exhaust gases reading for CO and CO_2 during the experiment were 1289 ppm and 32.5 %, respectively. In other words, incomplete combustion occurs during this experiment.

Case # 2: Gaseous fuel using 90 g nickel powder

In this case, in order to improve the combustion process, 90 g of nickel powder was used in the experimental work. The nickel powder was used as an oxygen carrier for complete combustion in the system under investigation. The results are shown in Figure 13. From this figure, it is clear that at the beginning, the CO concentration decreases until 400 s and it begins to increase; otherwise, the CO_2 concentration increases until 400 s and it begins to decrease. In other words, the combustion process was enhanced during this experiment. The average experimental exhaust gases reading for CO and CO_2 were 678.5 ppm and 48 %, respectively. The results also showed the effect of using oxygen carriers on combustion gases where the average ratio of the carbon monoxide was lower than that in Case #1.

Case #3: Gaseous fuel using 135 g nickel powder with supplementation

In this case, gaseous fuel was used using 135 g nickel powder and 45 g was added in the experiment. The additional amount of nickel powder was added to study the effect of nickel powder supply on the combustion process. The additional amount of nickel powder was added after five minutes, which is the time in which CO and CO_2 curves began to change its direction in the previous experiment. Figure 14 represents the concentrations of CO and CO_2 emissions for this case. From the analysis of this figure, it can be noticed that the average exhausts gases reading for CO and CO_2 were 655 ppm and 54.1 %, respectively. According to previously obtained data, it can be concluded that there is a significant difference in the readings of the combustion gases before and after using nickel powder.

The average carbon monoxide before using nickel powder was about 1289 ppm, and after using nickel powder, it decreased to 655 ppm, meaning that using metal powder decreases the rate of CO with an average value of 49.1 %. In addition, for carbon dioxide, the average value before using nickel powder was about 32.5 % and after using nickel powder, it was 54.1 %, meaning that using metal powder improves the rate of CO_2 by 66.5 % and improves the combustion process.

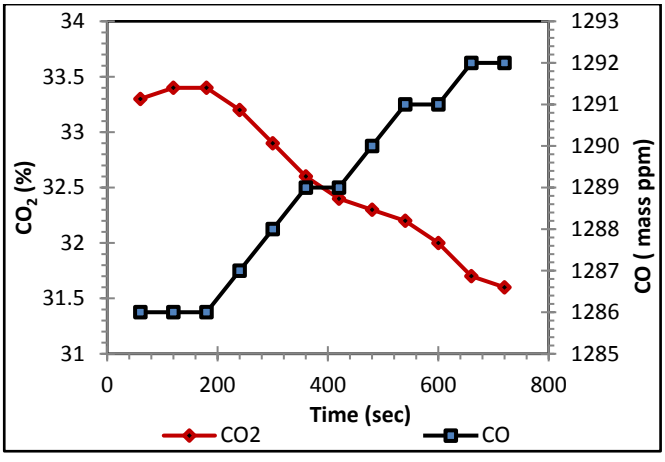

Figure 12. Concentrations of CO and CO_2 emissions for gaseous fuel without using metal powder

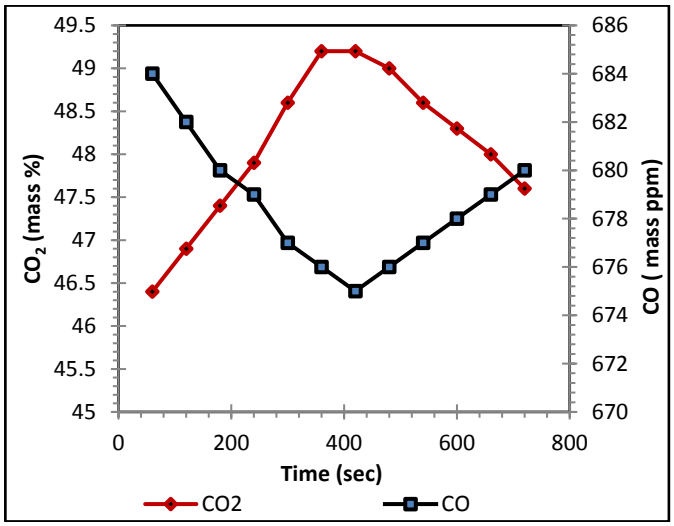

Figure 13. Concentrations of CO and CO_2 emissions for gaseous fuel using 90 g nickel powder

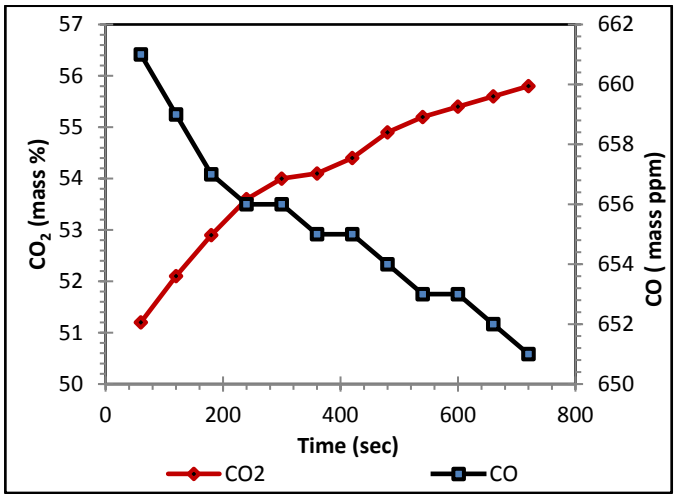

Figure 14. Concentrations of CO and CO_2 emissions for gaseous fuel using 135 g nickel powder with 45 g supplementation after five minutes

4.1.5. The effect of using nickel powder for gaseous fuel

As discussed in the previous section, nickel powder improved the combustion process. Thus, the temperature distribution along the fuel reactor was measured and recorded using experimental and numerical methods, as shown in Figures 15 and 16, respectively. From these figures, it is clear that there is an increase in the temperature after using oxygen carriers and the maximum recorded temperature is 1154 ºC and measured by T_1. A comparison between the temperature distribution for LPG fuel with and without using nickel powder is shown in Figure 17. This figure shows that the nickel powder increases the temperature distribution along the fuel reactor. Also, the flame color is essential to a better understanding of the complete or incomplete combustion process. Figure 18 shows the flame color with and without using nickel powder. From the photograph in Figure 18 (a), it is clear that the flame color is yellow and this is one of the common colors for incomplete combustion, indicating that after using nickel powder, complete combustion is very close. On the contrary, the flame color is blue when using nickel powder, meaning that when burning LPG with using nickel powder, the complete combustion process occurs, as shown in Figure 18 (b).

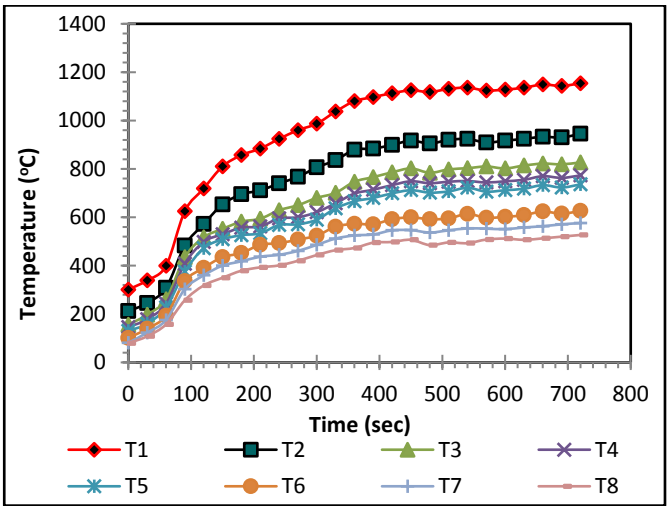

Figure 15. Experimental temperature distribution along the fuel reactor for LPG using nickel powder

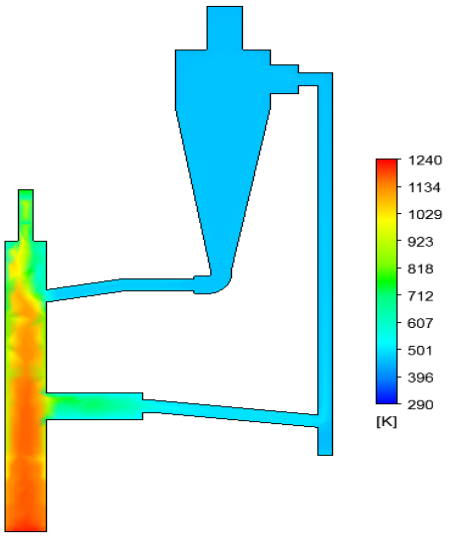

Figure 16. Simulated results of temperature distribution along the fuel reactor for LPG using nickel powder

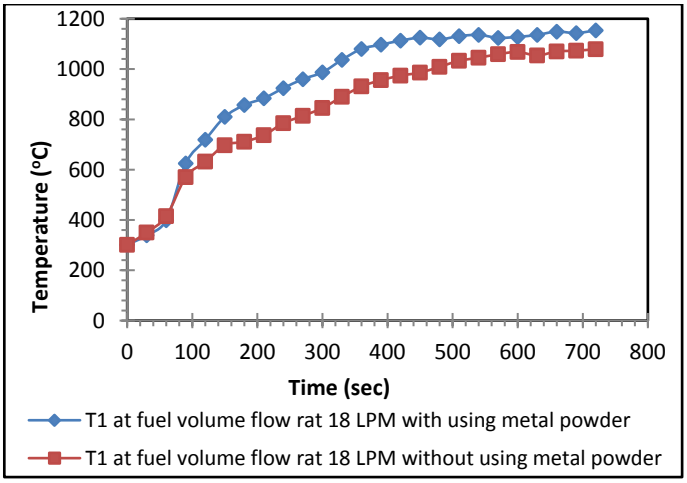

Figure 17. Comparison between the temperature distribution for LPG fuel with and without using nickel powder

(a) Without using nickel powder

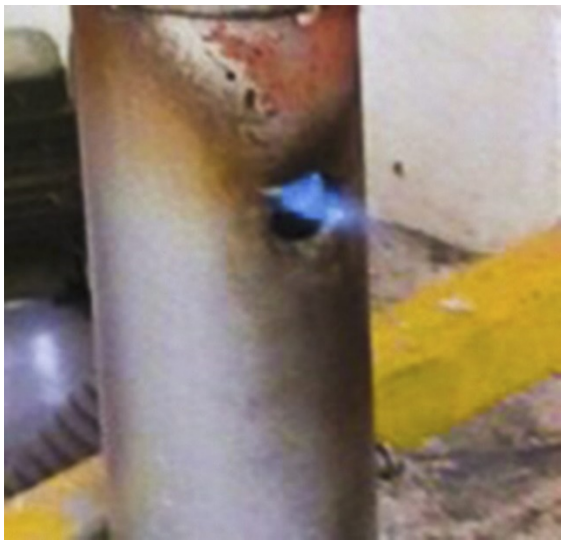

(b) With using nickel powder

Figure 18. The flame color of gaseous fuel with and without using nickel powder

4.2. Solid fuel (brown coal)

4.2.1. Experimental and simulated results for different brown coal diameters, without using nickel powder

For brown coal (1-2 cm diameter), the results are shown in Figure 19. The maximum recorded temperature was 422 ºC at T_1 and the temperature gradually decreased to 115 ºC at T_8. Figure 20 shows the results of temperature distribution along the fuel reactor for brown coal (2-3 cm diameter) without using nickel powder. From the analysis of this figure, it can be noticed that the maximum recorded temperature was 531 ºC at T_1 and the temperature gradually decreased to 129 ºC at T_8. Also, Figure 21 shows the experimental results of temperature distribution along the fuel reactor for brown coal (3-4 cm diameter) without using nickel powder. The maximum recorded temperature was 678 ºC at T_1 and the temperature gradually decreased to 159 ºC at T8. Figure 22 shows the temperature distribution along the fuel reactor for brown coal (4-5 cm diameter) without using nickel powder. From this figure, it is clear that the maximum recorded temperature was 840 ºC at T_1 and the temperature decreased gradually to 209 ºC at T_8. For brown coal (5-6 cm diameter), the results are shown in Figure 23. The maximum recorded temperature was 567 ºC at T_1 and the temperature gradually decreased to 218 ºC at T_8. The simulated results of temperature distribution for different brown coal diameters without using nickel powder are shown in Figure 24.

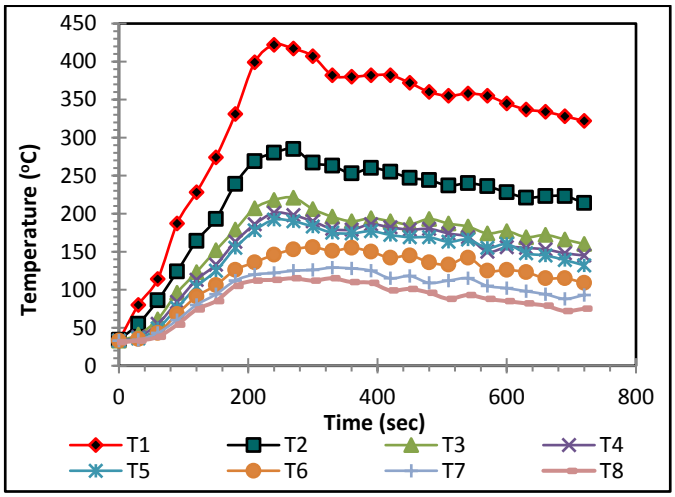

Figure 19. Experimental results of temperature distribution along the fuel reactor for brown coal (1-2 cm diameter) without using nickel powder

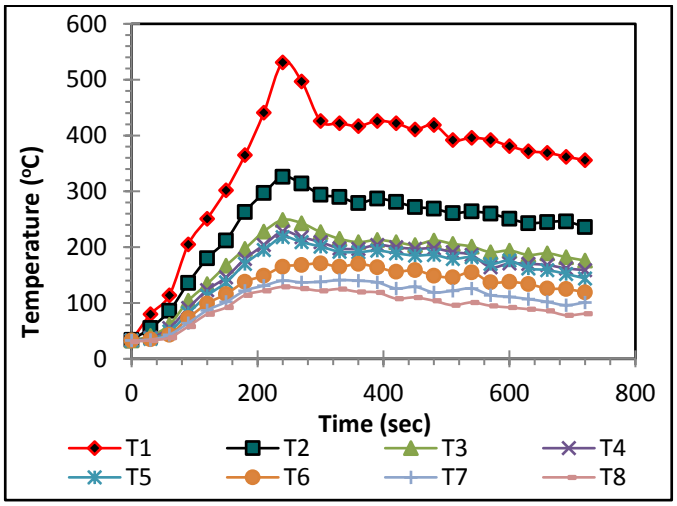

Figure 20. Experimental results of temperature distribution along the fuel reactor for brown coal (2-3 cm diameter) without using nickel powder

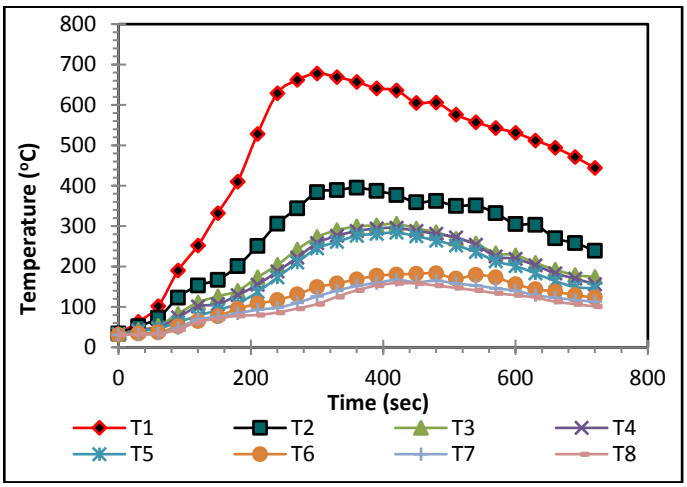

Figure 21. Experimental results of temperature distribution along the fuel reactor for brown coal (3-4 cm diameter) without using nickel powder

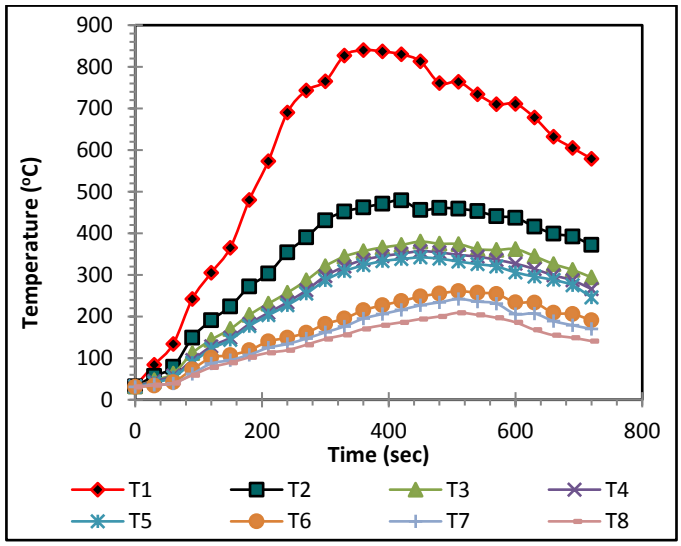

Figure 22. Experimental temperature distribution along the fuel reactor for brown coal (4-5 cm diameter) without using nickel powder

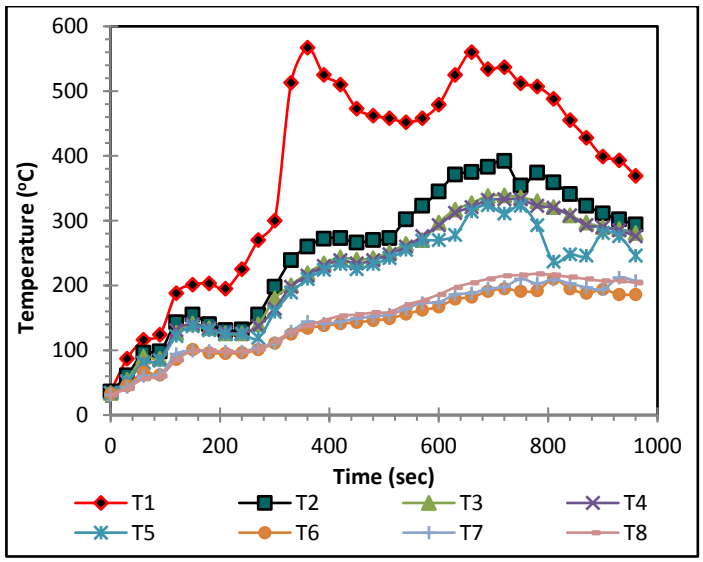

Figure 23. Experimental results of temperature distribution along the fuel reactor for brown coal (5-6 cm diameter) without using nickel powder

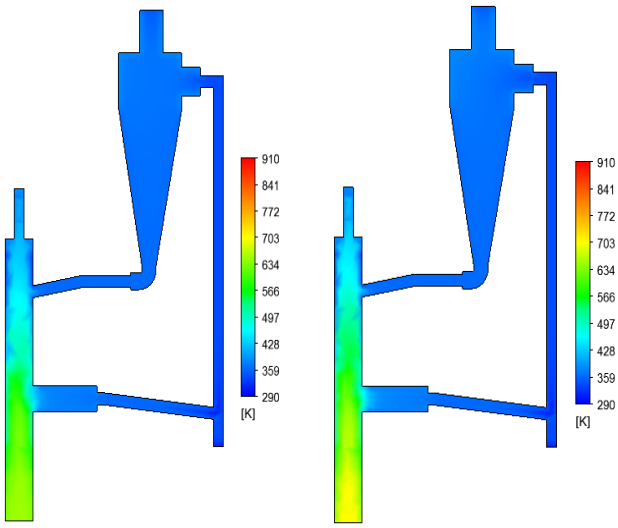

(a) Diameter from 1-2 cm (b) Diameter from 2-3 cm

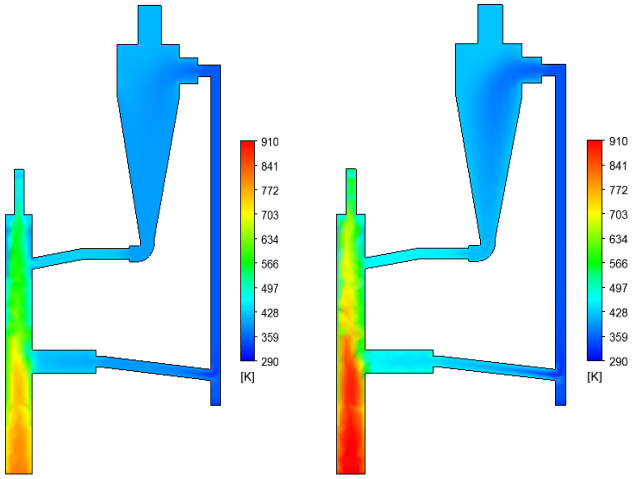

(c) Diameter from 3-4 cm (d) Diameter from 4-5 cm

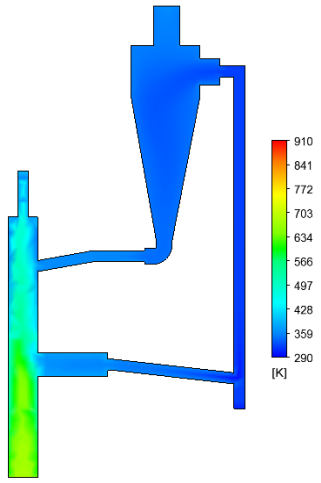

(e) Diameter from 5-6 cm

Figure 24. Simulated results of temperature distribution for different brown coal diameters without using nickel powder

4.2.2. Comparison between experimental and simulated results for different brown coal diameters

A comparison between the experimental results of temperature distribution in the combustion chamber (T_1) for different brown coal diameters is shown in Figure 25. From this figure, it is clear that the brown coal with a diameter (4-5 cm) gives the highest value of temperature distribution among the other diameters. Figure 26 shows the simulated results of temperature distribution along the fuel reactor for different diameters of brown coal. Also, the red region for the brown coal diameter of (4-5 cm) extends to a larger area, compared with the other diameters. It was observed that 4-5 cm diameter would be perfect and the temperature at the beginning of these experiments was less than the requirement of the reduction process of nickel powder.

Therefore, it is necessary to preheat the fuel reactor before starting the combustion process. The temperature at the beginning of the experiment is sufficient for nickel powder reduction. The experimental results of the temperature distribution with the preheated reactor are shown in Figure 27. From the analysis, it can be concluded that there was a significant increase in the temperature gradient and the maximum recorded temperature in this experiment was 973 °C at T_1. For this reason, all experiments for solid fuel were carried out with a 4-5 cm diameter and after preheating

the fuel reactor. Figure 28 shows the simulated temperature distribution along the fuel reactor for brown coal (4-5 cm diameter) upon preheating the fuel reactor.

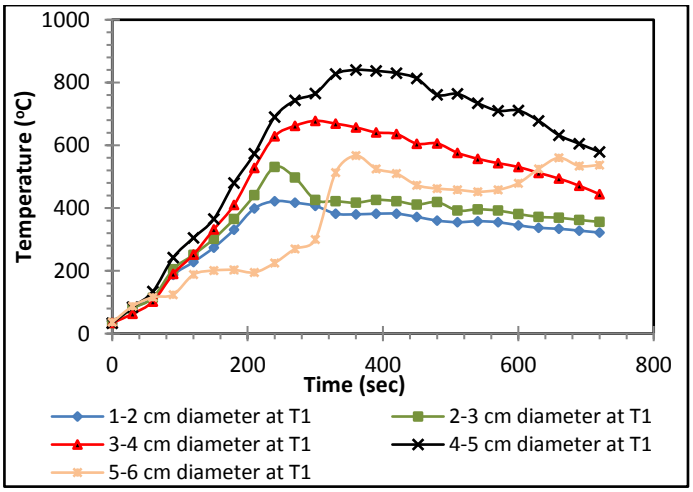

Figure 25. Comparison between the temperature distributions in the combustion chamber (T1) for different brown coal diameters

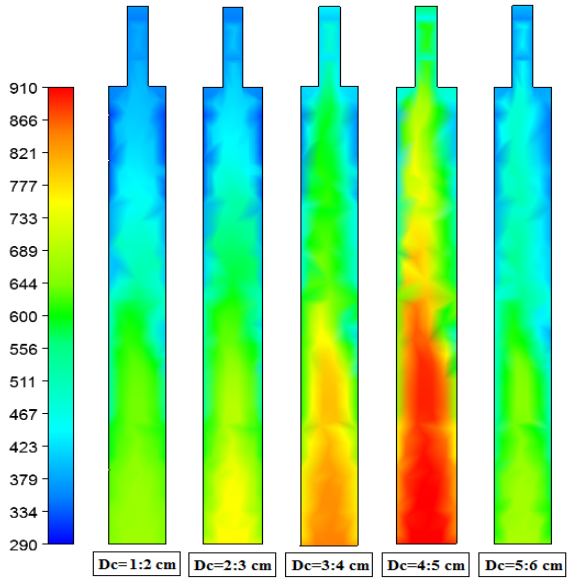

Figure 26. Simulated results of temperature distribution along the fuel reactor with different diameters of brown coal

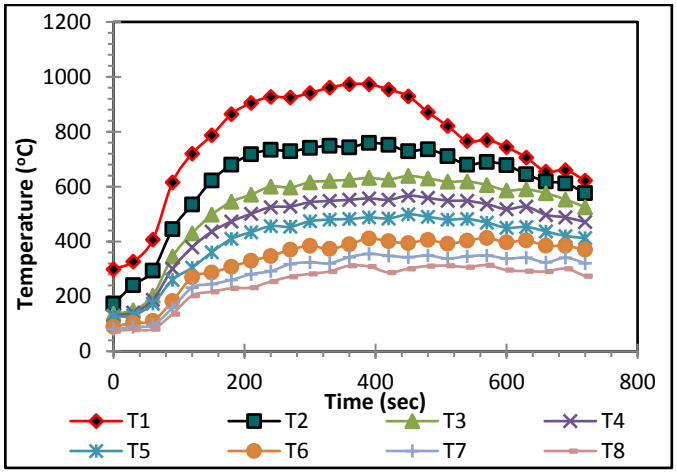

Figure 27. Experimental temperature distribution along the fuel reactor for brown coal (4-5 cm diameter) preheated reactor without using nickel powder

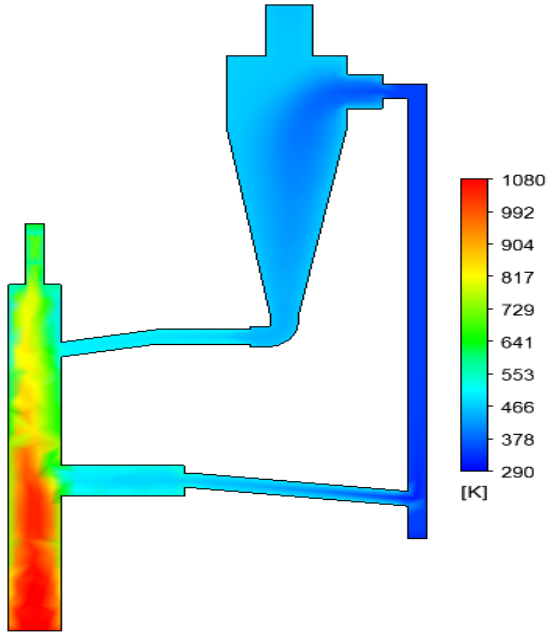

Figure 28. Simulated results of temperature distribution for brown coal (4-5 cm diameter), preheated reactor without using nickel powder

4.2.3. Validation for using brown coal without nickel powder

Figure 29 shows a comparison between experimental and simulated results for preheated fuel reactor using brown coal without using nickel powder. The brown coal has a diameter of 4-5 cm. From the analysis of this figure, it can be concluded that the values for the experimental results are consistent with those for the simulated results. The coefficient of determination (R^2) for the experimental and simulated results values of the brown coal equals 82.9 %.

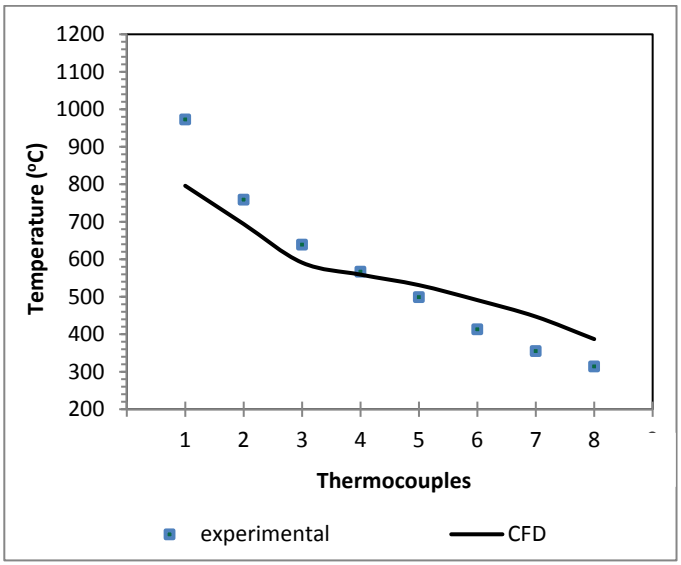

Figure 29. Experimental and simulated results of temperature distribution for brown coal, preheated reactor without using nickel powder

4.2.4. Experimental concentrations of CO and CO_2 for solid fuel

Table 8 shows the operating conditions of carbon monoxide and carbon dioxide Concentrations measurement for different cases with using solid fuel (brown coal).

Table 8. Operating conditions of CO and CO_2 concentrations of measurement experiments using brown coal fuel

Case	Combustion method	The reactor used in combustion	The used amount of nickel
Solid fuel (4-5 cm diameter of brown coal)			
Case # 1	Conventional combustion	The fuel reactor after separating it from the air reactor	without using nickel powder
Case # 2	CLC combustion technology	CLC system (fuel reactor and air reactor)	40 g
Case # 3			60 g and 20 g supplementation

Case # 1: Solid fuel, without using nickel powder

The concentration measurements of CO and CO_2 for solid fuel are discussed in three cases. In this case, the measurements were done without using nickel powder and the behavior of CO and CO_2 concentration is shown in Figure 30. This figure shows that the concentration of carbon monoxide increased continuously until the end of the experiment. In contrast, the concentration of carbon dioxide decreased significantly throughout the experiment, and the average exhaust gases reading for CO and CO_2 was 2591 ppm and 18.5 %, respectively.

Case # 2: Solid fuel, using 40 g nickel powder

In this case, 40 g of nickel powder was added to the fuel reactor. The concentrations of CO and CO_2 emissions were measured, as plotted in Figure 31. From the analysis of this figure, it can be concluded that using nickel powder as oxygen carrier improved the combustion process and the average exhaust gases reading of CO and CO_2 emissions were 1517 ppm and 26.8 %, respectively.

Case # 3: Solid fuel, using 60 g of nickel powder with supplementation

The effect of adding nickel powder with supplementation was studied in this case. In this experiment, 60 g of nickel was used at the beginning of the experiment and 20 g supplementation after six minutes. This time duration is the time at which the behavior of the curve begins to change its direction, as shown in Figure 32. From the analysis, it is clear that the CO_2 curve begins to increase significantly from the beginning to the end of the experiment. The average exhaust gases reading of the experiment for CO and CO_2 emissions was 1200 ppm and 31.8 %, respectively. According to the previously recorded data, there is a significant difference in the readings of the combustion gases before and after using nickel powder. The average carbon monoxide before and after using nickel powder was 2591 ppm and 1200 ppm respectively, meaning that using metal powder reduced the average rate of CO by 53.7 %. Also, the average carbon dioxide before and after using nickel powder was 18.5 % and 31.8 %, respectively, and this means that using metal powder improves the average rate of CO_2 by 71.9 %.

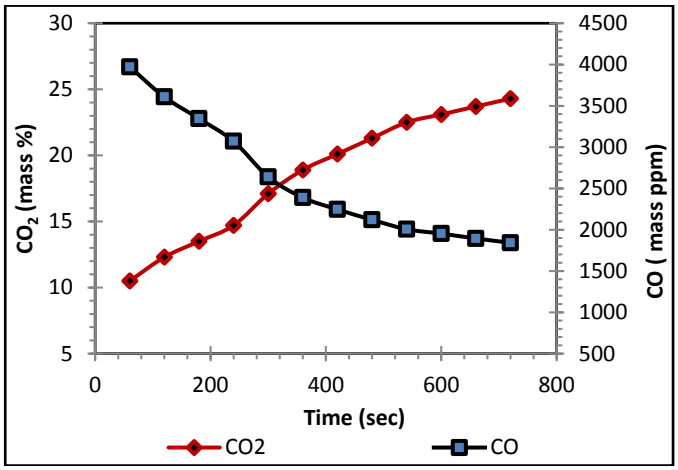

Figure 30. Concentrations of CO and CO_2 emissions for solid fuel without using metal powder

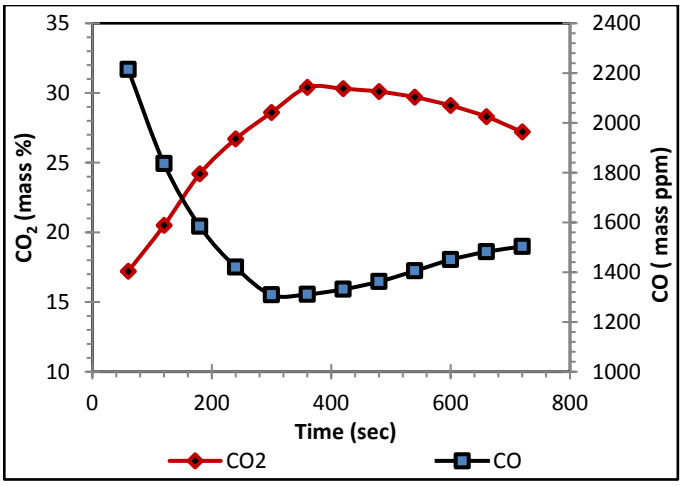

Figure 31. Concentrations of CO and CO_2 emissions using solid fuel with 40 g nickel powder

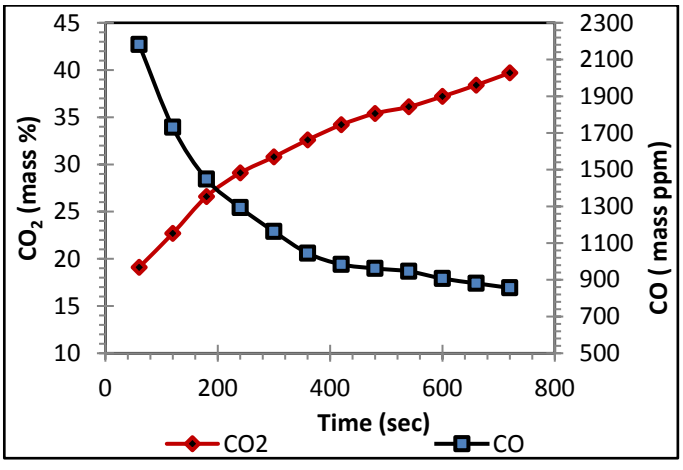

Figure 32. Concentrations of CO and CO_2 emissions using solid fuel with 60 g nickel powder and 20 g supplementation after six minutes

4.2.5. The effect of using nickel powder for brown coal fuel

The temperature distribution along the fuel reactor was measured and recorded using experimental and numerical methods, as shown in Figures 33 and 34, respectively. From these figures, it is clear that using oxygen carriers increases the temperature distribution. The maximum recorded

temperature was 1037 ºC at T1. The comparison between the temperature distribution for brown coal (4-5 cm diameter) with and without using nickel powder is shown in Figure 35. Also, it is clear that there is a significant increase in temperature which yields increase in the CO_2 percentage and the approach to the complete combustion process.

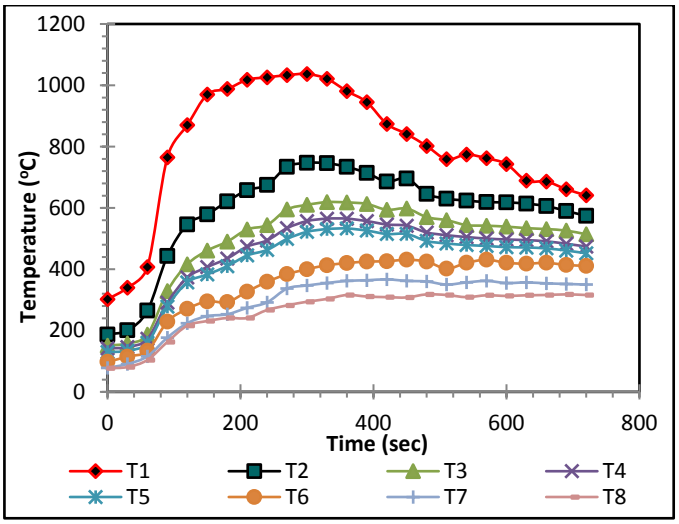

Figure 33. Temperature distribution along the fuel reactor for brown coal (4-5 cm diameter), a preheated reactor with nickel powder

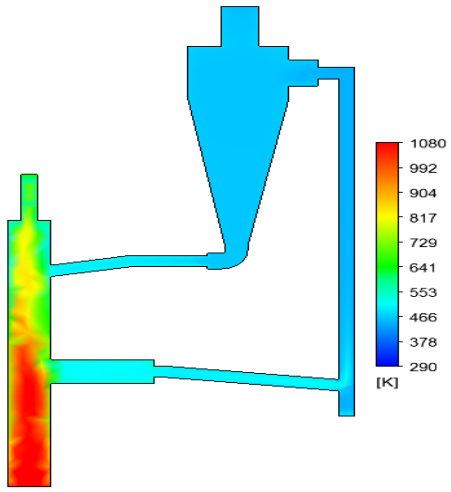

Figure 34. Simulated results of temperature distribution for brown coal (4-5 cm diameter), a preheated reactor with nickel powder

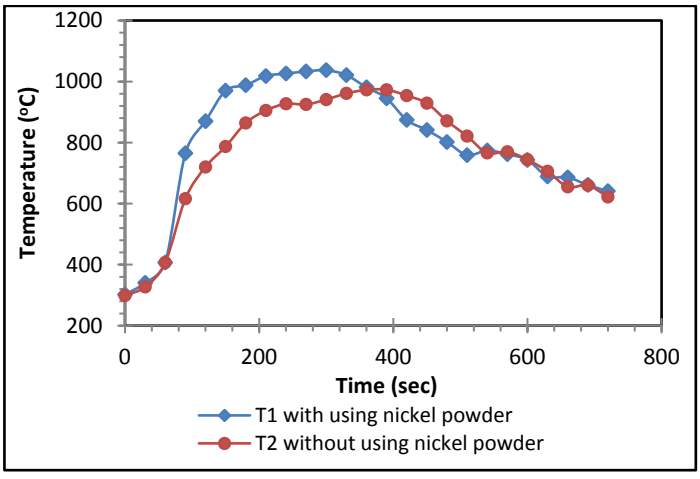

Figure 35. Comparison between the temperature distribution for brown coal (4-5 cm diameter) with and without using nickel powder

5. CONCLUSIONS

Chemical looping combustion is one of the most effective techniques that does not waste energy during the separation process of CO_2. In this study, a Chemical Looping Combustor (CLC) was designed and fabricated using nickel powder, brown coal and liquefied petroleum gas as an oxygen carrier. The temperature distribution along the fuel reactor using gaseous and solid fuels before and after applying CLC technology was investigated. The CO and CO_2 concentrations at combustion gases with and without using nickel powder were conducted for LPG and brown coal fuels. The temperature distributions along the fuel reactor for LPG flow rates of 11 and 18 LPM with and without using nickel powder as well as using preheated reactor were discussed and evaluated.

Also, the experimental results of temperature distribution along the fuel reactor for brown coal of different diameters with and without using nickel powder were studied. In addition a mathematical model was developed to simulate the combustion in CLC using combustion and energy code for both gas and solid phases. The experimental and simulated results were validated according to the coefficient of determination R^2. The results showed that the chemical looping combustion technique could be used for gaseous and solid fuels. Using nickel powder improved the combustion process and in case of using LPG, the color of the flame changed to blue which is the color of the complete combustion flame. The CO was reduced by 49.1 % and CO_2 increased by 66.5 %. In case of using brown coal as solid fuel, CO was reduced by 53.7 % and CO_2 was augmented by 71.9 %. Finally, there was good agreement between the experimental and simulated results based on the determination coefficient.

6. ACKNOWLEDGEMENT

The authors thank the combustion laboratory workers, Department of Mechanical Engineering, Faculty of Engineering, Suez Canal University, for technical guidance and support towards the preparation of this work.

REFERENCES

1. Karl, R. and Trenberth, K., "Modern global climate change", ***Science***, Vol. 302, (2003), 1719-1723. (https://doi.org/10.1126/science.1090228).
2. Chan., E.Y., "Climate change is the world's greatest threat–In Celsius or Fahrenheit", ***Journal of Environmental Psychology***, Vol. 60, (2018), 21-26. (https://doi.org/10.1016/j.jenvp.2018.09.002).
3. Pelletier, C., Rogaume, Y., Dieckhoff, L., Bardeau, G., Pons, M.-N. and Dufour, A., "Effect of combustion technology and biogenic CO_2 impact factor on global warming potential of wood-to-heat chains", ***Applied Energy***, Vol. 235, (2019), 1381-1388. (https://doi.org/10.1016/j.apenergy.2018.11.060).
4. IPCC, ***IPCC special report: Carbon dioxide capture and storage***, (2005). (Accessed: 10 July 2016) (https://www.ipcc.ch/report/carbon-dioxide-capture-and-storage/).
5. Cho, P., Mattisson, T. and Lyngfelt, A., "Comparison of iron-, nickel-, copper and manganese-based oxygen carriers for chemical-looping combustion", ***Fuel***, Vol. 83, (2004), 1215-1225. (https://doi.org/10.1016/j.fuel.2003.11.013).
6. Lyngfelt, A., Leckner, B. and Mattisson, T., "A fluidized-bed combustion process with inherent CO_2 separation; Application of chemical looping combustion", ***Chemical Engineering Science***, Vol. 56, (2001), 3101-3113. (https://doi.org/10.1016/S0009-2509(01)00007-0).
7. Ma, J., Zhao, H., Tian, X., Wei, Y., Zhang, Y. and Zheng, C., "Continuous operation of interconnected fluidized bed reactor for chemical looping combustion of CH_4 using hematite as oxygen carrier",

Energy Fuels, Vol. 29, (2015), 3257-3267. (https://doi.org/10.1021/ef502881x).

8. Linderholm, C. and Schmitz, M., "Chemical-looping combustion of solid fuels in a 100 kW dual circulating fluidized bed system using iron ore as oxygen carrier", ***Journal of Environmental Chemical Engineering***, Vol. 4, (2016), 1029-1039. (https://doi.org/10.1016/j.jece.2016.01.006).
9. Pérez-Vega, R., Abad, A., García-Labiano, F., Gayán, P., Luis, F. and Adánez, J., "Coal combustion in a 50 kWth chemical looping combustion unit: Seeking operating conditions to maximize CO_2 capture and combustion efficiency", ***International Journal of Greenhouse Gas Control***, Vol. 50, (2016), 80-92. (https://doi.org/10.1016/j.ijggc.2016.04.006).
10. Lewis, W.K., Gilliland, E.R. and Sweeney, W.P., "Gasification of carbon metal oxides in a fluidized power bed", ***Chemical Engineering Progress***, Vol. 47, (1951), 251-256. (https://doi.org/10.1021/ie50474a017).
11. Ishida, M. and Jin, H., "A novel combustor based on chemical-looping combustion reactions and its reactions kinetics", ***Journal of Chemical Engineering of Japan***, Vol. 27, (1994), 296-301. (https://doi.org/10.1252/jcej.27.296).
12. Lyngfelt, A. and Mattisson, T., "Materials for chemical-looping combustion", ***Process Engineering for CCS Power Plants***, (2011), 475-504. (https://www.worldcat.org/title/process-engineering-for-ccs-power-plants/oclc/740976968).
13. Lyngfelt, A., "Oxygen carriers for chemical looping combustion - 4000 h of operational experience", ***Oil & Gas Science and Technology***, Vol. 66, (2011), 161-172. (https://doi.org/10.2516/ogst/2010038).
14. Hoteit, A., Forret, A., Pelletant, W., Roesler, J. and Gauthier, T., "Chemical-looping combustion with different types of liquid fuels", ***Oil & Gas Science and Technology***, Vol. 66, (2011), 193-199. (https://doi.org/10.2516/ogst/2010022).
15. Moldenhauer, P., Ryd´en, M., Mattisson, T. and Lyngfelt, A., "Chemical-looping combustion and chemical-looping with oxygen uncoupling of kerosene with Mn- and Cu-based oxygen carriers in a circulating fluidized-bed 300 W laboratory reactor", ***Fuel Processing Technology***, Vol. 104, (2012), 378-389. (https://doi.org/10.1016/j.fuproc.2012.06.013).
16. Leion, H., Mattisson, T. and Lyngfelt, A., "The use of petroleum coke as fuel in chemical-looping combustion", ***Fuel***, Vol. 86, (2007), 1947-1958. (https://doi.org/10.1016/j.fuel.2006.11.037).
17. Jerndal, E., Mattisson, T. and Lyngfelt, A., "Thermal analysis of chemical-looping combustion", ***Chemical Engineering Research and Design***, Vol. 84, (2006), 795-806. (https://doi.org/10.1205/cherd05020).
18. Ishida, M., Jin, H. and Okamoto, T., "A fundamental study of a new kind of medium material for chemical-looping combustion", ***Energy Fuel***, Vol. 10, (1996), 958-963. (https://doi.org/10.1021/ef950173n).
19. Nakano, Y., Iwamoto, S., Maeda, T., Ishida, M. and Akehata, T., "Characteristics of reduction and oxidation cycle process by use of a Fe_2O_3 medium", ***Iron Steel J Jpn***, Vol. 72, (1986), 1521-1528.
20. Jin, H. and Ishida, M., "Reactivity study on natural-gas-fuelled chemical looping combustion by a fixed-bed reactor", ***Industrial & Engineering Chemistry Research***, Vol. 41, (2002), 4004-4007. (https://doi.org/10.1021/ie020184l).
21. Mattisson, T., Lyngfelt, A. and Cho, P., "The use of iron oxide as oxygen carrier in chemical-looping combustion of methane with inherent separation of CO_2", ***Fuel***, Vol. 80, (2001), 1953-1962. (https://doi.org/10.1016/S0016-2361(01)00051-5).
22. Mattisson, T., Järdnäs, A. and Lyngfelt, A., "Reactivity of some metal oxide supported on alumina with alternating methane and oxygen application for chemical-looping combustion", ***Energy Fuels***, Vol. 17, (2003), 643–651. (https://doi.org/10.1021/ef020151i).
23. Coleman, H.W. and Glenn Steele, W., Experimentation and uncertainty analysis for engineers, Wiley, New York, (1999). (https://www.wiley.com/en-us/Experimentation%2C+Validation%2C+and+Uncertainty+Analysis+for+Engineers%2C+4th+Edition-p-9781119417514).
24. Holman, J.P., Experimental method for engineers, 6th ed., McGraw-Hill, Singapore, (1994). (https://www.amazon.com/Experimental-Methods-Engineers-J-Holman/dp/0070296669).
25. Ismail, T.M., Ramzy,K., Abelwhab, M.N., Elnaghi, B.E., Abd El-Salam, M. and Ismail, M.I., "Performance of hybrid compression ignition engine using hydroxy (HHO) from dry cell", ***Energy Conversion and Management***, Vol. 155, (2018), 287-300. (https://doi.org/10.1016/j.enconman.2017.10.076).
26. Yaws, C.L. and Braker, W., "Flammability characteristics of combustible gases and vapors", Matheson gas data book, New York: Parsippany, NJ: Matheson Tri-Gas, Vol. 443, (2001). (https://www.worldcat.org/title/matheson-gas-data-book/oclc/46685585).
27. Koshiba, Y., Hasegawa, T., Kim, B. and Ohtani, H., "Flammability limits, explosion pressures, and applicability of Le Chatelier"s rule to binary alkane–nitrous oxide mixtures", ***Journal of Loss Prevention in the Process Industries***, Vol. 45, (2017), 1-8. (https://ynu.repo.nii.ac.jp/?action=repository_action_common_download&item_id=9396&item_no=1&attribute_id=20&file_no=1).
28. Maindonald, J. and Braun, J., Data analysis and graphics using R: An example-based approach, Cambridge University Press, (2006). (https://www.amazon.com/Data-Analysis-Graphics-Using-Example-Based/dp/0521762936).